Molecular Modeling Studies of the DNA−Topoisomerase I Ternary Cleavable Complex with Camptothecin

Y. Fan, J. N. Weinstein,* K. W. Kohn, L. M. Shi, and Y. Pommier*

Laboratory of Molecular Pharmacology, Division of Basic Sciences, National Cancer Institute, Building 37, Room 5D02, National Institutes of Health, Bethesda, Maryland 20892-4255

Received July 25, 1996

The present studies provide a three-dimensional model for the postulated ternary cleavable complex of topoisomerase I (top1), DNA, and camptothecin (CPT). Molecular simulations were done using the AMBER force field. The results suggest that a ternary cleavable complex might be stabilized by several hydrogen bonds in the binding site. In this proposed "drug-stacking" model, CPT is pseudointercalated in the top1-linked DNA cleavage site and interacts with the protein near its catalytic tyrosine through hydrogen bonding and stacking. The structural model is consistent with the following experimental observations: (i) the N3 position of the 5′ terminal purine of the cleaved DNA strand is readily alkylated by 7-chloromethyl 10,11-methylenedioxy CPT; (ii) CPT generally tolerates substituents at positions 7, 9, and 10 but is inactivated by additions at position 12; (iii) 10,11-methylenedioxy (MDO) CPT is much more potent than 10,11-dimethoxy (DMO) CPT; (iv) the lactone portion of CPT is essential for top1 inhibitory activity; (v) 20*S* derivatives of CPT are much more potent than the 20*R* analogues; (vi) a catalytic tyrosine hydroxyl in top1 covalently links to the 3′ terminal base, T, of the cleaved DNA strand; and (vii) top1 mutation Asn722Ser leads to CPT resistance. A total of 18 camptothecin derivatives with different DNA cleavage potencies were docked into the hypothetical cleavable complex binding site to test and refine the model. These studies provide insight into a possible mechanism of top1 inhibition by CPT derivatives and suggest rational approaches for the design of new CPT derivatives.

Introduction

DNA topoisomerase 1 (top1) is an enzyme essential for relaxation of DNA during a number of critical cellular processes, including replication, transcription, and repair.[1−3] Top1 catalyzes changes in the linking number of DNA by breaking and resealing phosphodiester bonds. In contrast to topoisomerase II, which induces both single- and double-strand breaks, top1 mediates only single-strand breaks.[1−4] The top1-mediated reaction can be divided into four steps: (1) enzyme−DNA binding; (2) DNA single-strand cleavage by reversible transesterification, in which the 5′ oxygen of a phosphodiester bond is exchanged for the hydroxyl group on tyrosine 723 of human top1 (through which the protein becomes covalently linked to the 3′ terminus of the cleaved DNA strand); (3) single-strand passage; (4) re-ligation of the cleaved DNA strand.

Top1 is a cellular target for anticancer drug development, and the best characterized top1 inhibitors are camptothecin (CPT) and its derivatives.[4−6] Renewed interest in this class of compounds is due primarily to their activity against a broad range of tumors and the identification of several promising CPT derivatives, including 9-amino CPT (NSC-603071), topotecan (NSC-609699), and CPT-11 (NSC-616348). These analogues have recently been introduced into the clinic.[7,8] Camptothecin binds only weakly to normal B-DNA under physiological conditions,[9] and it does not bind to top1 alone. CPT induces top1-linked DNA breaks by preventing DNA re-ligation. The intermediate in top1-linked DNA breakage is referred to as a "cleavable complex"[4,6] because it is readily reversible to a noncovalent enzyme−DNA complex before or after topoisomerization of the DNA. Experimental studies[10−12] suggest interaction of CPT with both the enzyme and the DNA, forming a ternary complex that stabilizes the transesterification intermediate. However, the structure of this complex remains to be determined. Present knowledge of CPT-induced complexes relies on enzyme mutation studies,[1] structure−activity studies of camptothecin derivatives,[1,13−15] DNA base sequence analyses,[12,16] and detailed examination of the drug's effects on different steps in the catalytic cycle.[17,18]

A stacking model has been proposed[12,16] for camptothecins on the basis of analyses of local DNA sequences around top1 sites. Approximately 90% of top1 sites have a T at position −1 whether CPT is present or not. By contrast, position +1 does not show significant preference in the absence of drug, but in the presence of CPT, guanine (G) is strongly preferred. These experiments suggest that CPT may interact with the base at the 5′ terminus of top1-induced DNA breaks and that the planar multiring system of CPT binds by stacking preferentially with G. This hypothesis provided a starting point for our modeling studies.

CPT analogues have been synthesized by numerous research groups, and the results of these efforts have been comprehensively reviewed.[1,13,14] These analogues provide the basis for our present understanding of the relationship between structure and activity, including substituent effects in the A and B rings and the role of

* To whom correspondence should be addressed. Phone: (301) 496-5944. Fax: (301) 402-0752.

S0022-2623(96)00544-4
Published on Web 05/20/1998

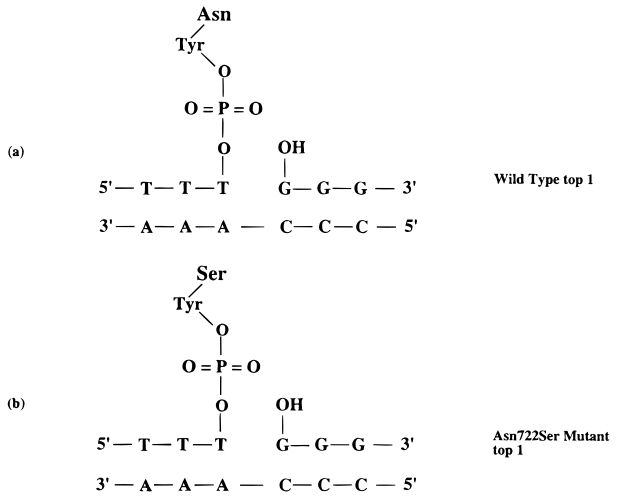

Figure 1. Schematic diagrams of hypothetical DNA−top1 complexes.

the E ring lactone in antitumor activity. It has been suggested that camptothecin might first bind noncovalently to the enzyme−DNA complex as the closed lactone form and that subsequent reversible lactone ring opening could stabilize the covalent complex.[19−21] The hypothesis that CPT links covalently to top1 is further supported by the observation that 20*S* CPT sodium salt and 21*S* lactam are essentially inactive.[14,15,22]

In this study, we used molecular mechanics methods to model possible ligand binding configurations in the top1−DNA complex (Figure 1). The extensive and varied nature of experimental evidence stimulated our attempt to find a plausible structural model. We have taken into account the following experimental observations: (i) 7-chloromethyl 10,11-MDO CPT leads to formation of an irreversible ternary cleavable complex with alkylation of the purine N3 at the 5′ DNA terminus;[11] (ii) CPT stabilizes a single-strand cleaved DNA complex with top1 covalently linked to the 3′ terminus[1−3] through a catalytic site tyrosine hydroxyl by transesterification, and the cleavage occurs preferentially between T and G (in the sequence 5′-TG-3′);[12,16,17] (iii) CPT generally tolerates substituents at positions 7, 9, and 10 but is inactivated by additions at position 12;[14,15,21,23−25] (iv) activity is retained when a methoxy group is added at either position 10 or 11; addition of a methylenedioxy group to form a five-membered ring across positions 10 and 11 (10,11-MDO CPT) enhances potency, while the simultaneous addition of methoxy groups to positions 10 and 11 (10,11-DMO CPT) is inactivating;[15] (v) the E ring lactone is essential for top1 inhibitory activity;[14,15,22,26] (vi) CPT has an asymmetric center at position 20, and its 20*S* configuration is active, but the 20*R* is essentially inactive;[15,26] and (vii) mutation Asn722Ser, adjacent to the reactive tyrosine in top1, allows the enzyme to retain activity but renders it resistant to CPT.[27]

We investigated whether these experimental findings could be accounted for on the basis of a computational model for the ternary cleavable complex. The mode of ligand binding in the complex was evaluated in terms of structure and energetics. We initially formulated the hypothetical model on the basis of CPT itself; subsequently, the model was further tested on the alkylation complex with 7-chloromethyl 10,11-MDO CPT AND six CPT analogues (2−4, 6, 13−15 in Figure 2). Later we studied 10 additional camptothecin analogues, including four substituted methylenedioxy and ethylenedioxy camptothecins[28,29] to provide additional tests. The model appears to be predictive for these molecules in terms of their quantitative activity profiles. However, precise theoretical estimation of binding affinities was limited by the lack of available crystallographic or NMR data for the eukaryotic top1. The present work provides a plausible three-dimensional "drug-stacking" model that may be useful in the structure-based design of top1 inhibitors for use in cancer chemotherapy.

Methods

The AMBER all-atom force field[30,31] was used for all energy calculations and minimizations. Molecular mechanics simulations were carried out on a Silicon graphics IRIS Indigo workstation using the SYBYL 6.2 graphics interface.[32] Bulk solvent effects on the electrostatic interactions were represented by a sigmoidal distance-dependent dielectric function. The energy convergence criterion used in final calculations for the structures of all complexes was 0.01 kcal/mol.

Camptothecin derivatives that contain functional groups not parametrized by the above force field required the derivation of parameters specific for each new bond, bond angle, and torsional angle type. To do so, we started with the existing parameters in the AMBER force field and reasonable "guess" values to do calculations for a set of small molecules. The geometries of these molecules were compared with structures calculated by a high level ab initio method (MP2/6-31G**) in the Gaussian 94 program on a host mainframe Convex C3830 supercomputer under Convex OS 10.2. The quantities were then optimized in an iterative process until the structures were deemed to be adequately fit. The existing AMBER force field was supplemented with these additional parameters for CPT ligands.

The docking procedure depended on two principal features: (1) an energy (or scoring) function for evaluating trial configurations of the two interacting molecules and (2) an algorithm for seeking the best achievable minimum of this function. A "rigid docking procedure" was used. The two interacting molecules were considered as rigid bodies, and the sum of the van der Waals and electrostatic energy terms was used as the scoring function. The possibility of hydrogen bond formation between the hypothetical receptor site and the ligand was also taken into account. The docking was optimized so as to avoid steric repulsions, increase favorable electrostatic interactions, and maximize hydrogen bonding pairs. "Monitor pairing", a Sybyl command to monitor the distance between pairs, was applied here to position ligands in a given hypothetical binding site according to the acceptable distances of hydrogen bonding and nonbonded interactions.

Hypothetical structures resulting from the initial docking were then energy-minimized. In early stages of minimization, the ligand variables were locked. Minimization was performed by successively decreasing the number of constraints. Finally, all variables were released, and minimization continued until the energy convergence criterion was reached. It made no significant difference in what order constraints were released. Structural and energetic features of the resulting complex were evaluated.

Results and Discussion

1. Hypothetical Receptor Site Model. Calculations were done for an assumed DNA fragment with six base pairs, 5′-T-T-T-G-G-G-3′, bound to the complementary sequence 3′-A-A-A-C-C-C-5′. Helicoidal coordinates were obtained from crystallographically derived fragments of the structure of B-DNA duplexes in the Sybyl 6.2 biopolymer module.[32] On the basis of the experimental hypothesis, a break was created between base-

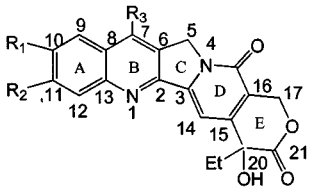

1: 20-S-CPT — R_1=H, R_2=H, R_3=H
2: 20-R-CPT — R_1=H, R_2=H, R_3=H
3: 10-NH_2, 11-OH 20-S-CPT — R_1=NH_2, R_2=OH, R_3=H
4: 10,11-DMO 20-S-CPT — R_1=OCH_3, R_2=OCH_3, R_3=H
5: 7-Et, 10-OH 20-S CPT (SN-38) — R_1=OH, R_2=H, R_3=Et

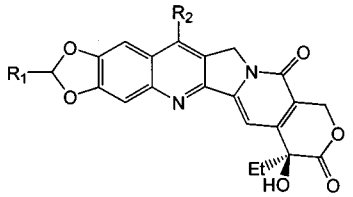

6: 10,11-MDO 20-S-CPT — R_1=H, R_2=H
7: 2-CH_2OH, 10,11-MDO-20S-CPT — R_1=CH_2OH, R_2=H
8: 2-CH_2NH_2 10,11-MDO-20S-CPT — R_1=CH_2NH_2, R_2=H
9: GI149893 — R_1=H, R_2=CH_2–N(CH)(CH)N–CH_3

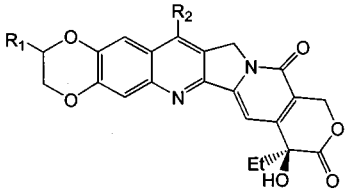

10: 2-CH_2OH 10,11-EDO-20S-CPT — R_1=CH_2OH, R_2=H
11: 2-CH_2NH_2 10,11-EDO-20S-CPT — R_1=CH_2NH_2, R_2=H
12: GI147211 — R_1=H, R_2=CH_2–N(CH)(CH)N–CH_3

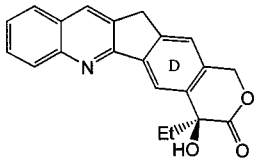

13: Ring D benzo-20-S-CPT

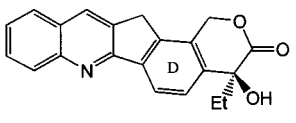

14: Ring D isobenzo-20-S-CPT

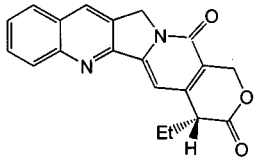

15: 20-deoxy-S-CPT

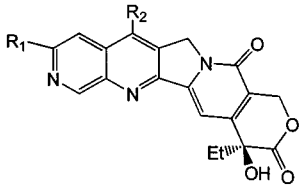

16: 7-Me, 10-CH_2NH_2 11-aza-20S-CPT — R_1=CH_2NH_2, R_2=Me
17: 7-Et, 10-H_2NC=NOH 11-aza-20S-CPT — R_1=H_2NC=NOH, R_2=Et
18: 7-Et, 10-H_2NC=NH 11-aza-20S-CPT — R_1=H_2NC=NH, R_2=Et

Figure 2. Camptothecin and camptothecin derivatives used in the modeling studies.

paired nucleotides T and G in the model DNA duplex. Two critical amino acid residues, Tyr723 and Asn722 of human top1, were attached to the cleaved strand of DNA at the 3′ terminus, and the models were built accordingly. Figure 1 shows hypothetical binding sites for DNA with wild-type top1 and the Asn722Ser mutant.

It has been reported that protein backbones typically undergo only minor distortions during binding, whereas the side chains may be subject to much larger conformational changes.[33,34] This assumption was adopted here to evaluate configurations of two amino acid residues, Tyr723 and Asn722 of human top1 in the complex. Camptothecin was chosen as the template molecule to determine the conformation of the peptide bond in the hypothetical binding site. One of the lowest energy conformations showing complementary fit between the binding site and the ligand (CPT) was adopted in modeling the ternary cleavable complex and was also assumed as the initial structure in the building of other complexes. Rationale for this hypothetical DNA−top1 binding site model was also provided by the experimental observation that a top1 mutated (Asn^{722} → Ser) next to the catalytic tyrosine (Tyr^{723}) is resistant to camptothecin.[27] The binding site was minimized in the AMBER force field until all calculated derivatives converged, with a criterion of 0.05 kcal/mol. Kollman charges were generated for approximating electrostatic interactions in the models.

2. Ligand Model and Conformational Analysis of 20 *S* CPT. A total of 18 camptothecin derivatives (see Figure 2) with different top1-induced DNA cleavage potencies were tested in this modeling study. The structures were built using the Sybyl graphics program and then minimized in AMBER with supplemental force field parameters. Charges on the ligands were computed by the AM1 semiempirical quantum mechanical method.

Conformational analysis of 20*S* CPT was done by the random search method in the Tripos Force Field.[32] A total of six conformers, including both "upboat" (carbonyl on ethyl side of CPT plane) and "downboat" (carbonyl on hydroxyl side of CPT plane) conformations, were found based on the energy cutoff 50 kcal/mol and on chirality checking. Each conformer was then fully energy-minimized using the AMBER force field, AM1 semiempirical method, and ab initio calculation using the STO-3G basis set. The results compiled in Table 1 show a general consistency between the AMBER force field method and other quantum mechanical calculations. Superimposing all six conformers, the CPT molecules were found to be quite rigid with the excep-

Table 1. Conformational Energies (kcal/mol) of 20*S* Camptothecin (CPT) Calculated by Different Methods

conformer	1[b]	2	3	4	5	6
AMBER[a]	0.33	3.09	5.77	5.68	4.66	0.00
AM1	0.00	3.35	4.58	4.14	4.42	0.54
STO-3G	0.03	3.62	4.07	4.84	4.79	0.00

[a] AMBER refers to the AMBER force field with supplemental parameters for CPT ligands. [b] Conformer **1** has essentially same conformation as the X-ray structures reported for two CPT derivatives.[34,35] This conformer was used in the docking studies.

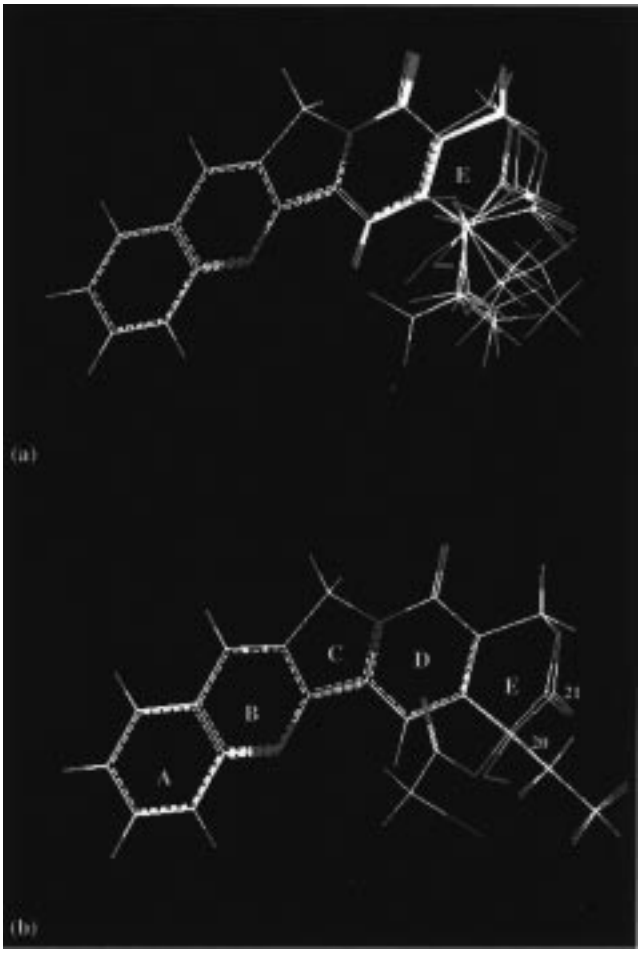

Figure 3. (a) Superimposition of the eight lowest-energy conformers of 20*S* CPT. (b) Superimposition of the minimized structure of conformer **1** and the X-ray structure of a CPT iodoacetate.[34]

tion of the E ring (see Figure 3a). The second most stable conformer (conformer 1) predicted in our AMBER force field was consistent with the structures of the two CPT derivatives whose X-ray structures have been reported to date.[24,35] Figure 3b shows the close structural correspondence between conformer 1 and one of these CPT derivatives (RMS = 0.09 Å).[35] The energy of this conformer was only marginally higher than that of the most stable one. In terms of both energetic and structural results, the AMBER force field, with the inclusion of additional parameters for CPT ligands, appeared adequate for calculations on this complex.

Conformer 1 of 20*S* CPT was assumed to be the major receptor-bound conformation in the ternary cleavable complex, and its enantiomer was, correspondingly, considered as the ligand conformation for 20*R* CPT. All other CPT derivatives were considered to adopt the same "core" conformation, but allowing the conformational flexibilities of the additional functional groups (such as dimethoxy groups on the A ring of 10,11-DMO CPT).

3. The Energy-Minimized Structure of the Ternary Cleavable Complex. 20*S* CPT was docked with the DNA−top1 binding site. We obtained a total of eight hypothetical ternary cleavable complex structures in the energy range of 16 kcal/mol according to different binding modes and locations. Among these, the "pseudointercalation" (or "drug-stacking") model shown in Figure 4 had the lowest energy. The energy difference between this model and next closest model was about 5 kcal/mol, and exploratory analysis indicated that it fitted the experimental evidence best. We therefore postulated the drug pseudointercalation binding site into which we could introduce other CPT analogues to investigate interactions. The interaction energies for association of DNA−top1 with different CPT analogues are compiled in Table 2, along with the corresponding anti-top1 activities and the calculated distances between associated hydrogen-bonding donors and acceptors. The model suggests that the interaction of CPT with DNA and top1 involves pseudointercalation between the base pairs of DNA flanking the top1 cleavage site. This insertion provides stacking forces between superposed and parallel aromatic fused rings. The nature of stacking interactions is not well understood; although electrostatic contributions and the dispersion portion of the van der Waals term of the empirical potential are reported to be the leading terms in the calculation of stacking forces,[36−38] important contributions[39−41] such as the so-called "p interactions" are still not included in the simple empirical potentials. Therefore, the estimated interaction energies shown in Table 2 do not reflect the stacking interaction fully. Additional stabilization of the complex is provided by hydrogen bonds between the DNA−top1 binding site and CPT molecule (see section 6).

Figures 4 and 8a show a model of the best energy-minimized CPT−DNA−top1 ternary cleavable complex. This CPK model provides an excellent "fit" and optimum numbers of hydrogen bonding pairs in the hypothetical binding site. The protein backbone of top1 extends toward the major groove of DNA. The camptothecin molecule is oriented with the E ring near the DNA break, and the concave portion of the drug molecule faces the DNA major groove. The model is consistent with the "drug-stacking" hypothesis[12,16,20] in which CPT forms hydrogen bond with the base at the DNA cleavage site and interacts with the protein near its catalytic tyrosine.[27] In the model, complex formation also induces conformational changes in the side chains of amino acids in the top1 that are close to the binding site. In other words, the structural evidence suggests an induced-fit mechanism for CPT−DNA−top1 interaction.

4. 7-Chloromethyl-MDO-CPT and B Ring Chemistry. Early studies showed that top1-linked DNA breaks are readily reversible and that CPT stabilizes the transesterification intermediate.[5,42] However, further topoisomerization of the DNA strands is still possible after the drug dissociates. To enhance stability of the ternary cleavable complex and determine the CPT

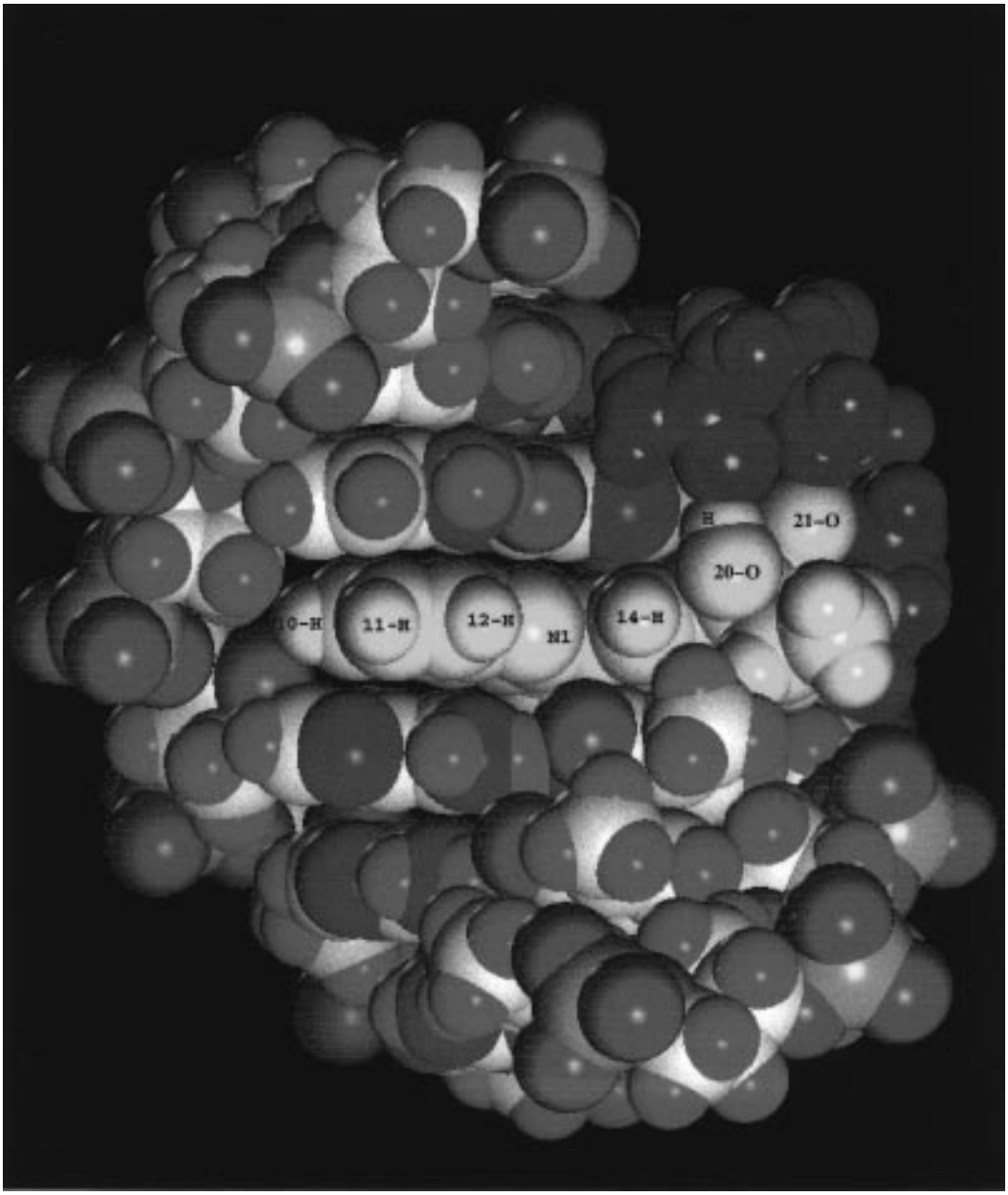

Figure 4. CPK model of the ternary cleavable complex structure viewed facing the DNA major groove (CPT docked): yellow, CPT (atoms and positions are indicated, and defined in Figure 2); violet, top1 (amino acids: Tyr723−Asn722).

binding site, CPT derivatives with an alkylating group have been synthesized.[10,11] An alkylating camptothecin derivative, 7-chloromethyl 10,11-methylenedioxycamptothecin (7-ClMe-MDO-CPT), was tested against mammalian top1 using a DNA oligonucleotide containing a single top1 cleavage site, and its activity was compared with that of its nonalkylating parent compound.[11,43] Alkylation of the N3 position of the +1 purine (adenine or guanine) by 7-ClMe-MDO-CPT in the presence of top1 cleavable complexes provided direct evidence that camptothecins inhibit top1 by binding at the enzyme−DNA interface.[11]

Given these observations, we asked whether the 7-ClMe-MDO-CPT alkylated to the +1 base would fit into the hypothetical binding site of our model. The modeling results indicated that 7-ClMe-MDO-CPT alkylation at the N3 position is possible. However, it is likely that another conformation of the drug−DNA−top1 complex exists for the alkylation transition state. The minimized final covalent alkylation model ("N3-complex") is shown in Figure 6. Only minor distortions were found for the "purine N3-complex" in comparison with the original noncovalent model.

Most substitutions at the 7-position of the B ring of CPT enhance top1 inhibition. This is clearly the case for compounds GI149893 and GI147211[25] (compounds 9 and 12 in Figure 2), as well as for SN-38, the active metabolite of CPT-11, which is in the clinic. When these 7-substituted CPTs were examined according to the model, they all showed more favorable interactions than did CPT itself.[44]

5. A Ring Chemistry. The structure−activity relationships of various camptothecin derivatives indicate that the two most distant rings of CPT (rings A and E) (see Figure 2) are critical for top1 inhibition. Although the present model is by no means able to draw a complete picture of the interaction of the A ring with

Table 2. Estimated Interaction Energies and Hydrogen-Bonding Interactions between Ligands and the Hypothetical Binding Site

complex[a]	top1 inhibition[b]	ref	E_{inter}[c]	H_1[d]	H_2[d]	H_3[d]	H_a[e]	H_b[e]	H_c[g]
1	+	16	−71.67	1.85	1.97	1.86			
2	−	16	−60.17	6.07	1.92	6.86			
3	++	42	−76.11	1.86	1.90	1.86			
4_2	−	16	−64.19	4.24	1.96	4.58			
4_4	−	16	−58.40	4.12	3.55	5.33			
4_5	−	16	−54.51	4.53	3.21	5.13			
5	+++	51	−85.63	1.90[f]	1.89	1.88			2.13
6	+++	16, 21	−75.79	1.85	2.00	1.86			
7	+++	28	−76.87	1.88	1.95	1.86			
8	+++	28	−78.08	1.89	1.94	1.86			
9	++	50	−76.75	1.86	1.97	1.86			
10	+++	27	−78.00	1.89	2.02	1.86	1.79		
11	+++	27	−81.71	1.89	2.02	1.86	1.79		
12	++	50	−77.51	1.87	1.98	1.85			
13	−	16	−69.24	1.89	1.94	1.86			
14	−	16	−67.99	1.93	−	1.92			
15	−	16	−65.14	−	1.93	1.88			
16	+	49	−73.25	1.88	1.96	1.86	1.97		
17	+++	49	−78.29	1.93	1.88	1.86	1.83		
18	+++	49	−79.71	1.93	1.86	1.88	1.83	2.66	
19	−	23	−69.46	−	2.00	1.94			

[a] Complexes **1**−**18** refer to the best energy-minimized structures of the model complex of wild-type top1 with the CPT ligands shown in Figure 2. Complex **19** indicates the best energy-minimized structure of the model complex of the Asn722Ser mutant top1 with CPT docked. [b] The signs refer to different top1-induced DNA cleavage activities (+, comparable to CPT; ++, more potent than CPT; +++, much more potent than CPT; −, inactive). [c] E_{inter}, the interaction energy, is represented by the equation, $E_{inter} = E_{complex} - E_{ligand\ f} - E_{site\ f}$, where $E_{ligand\ f}$ and $E_{site\ f}$ are the energies of the free ligand and site, respectively. [d] H_1 − H_3 refer to possible hydrogen-bonding pairs described in Figure 6. [e] These refers to the additional hydrogen-bonding pairs formed between the A ring and the oxygen of the sugar ring or phosphodiester bond. [f] 20-OH of SN-38 (compound **5** in Figure 2) is predicted to form a stronger hydrogen bond with the purine N3 at the 5′ DNA terminus than with the carbonyl oxygen of Asn722 of top1 (H1 shown in Figure 6). [g] 10-OH of SN-38 (compound **5** in Figure 2) forms another hydrogen bond with the oxygen of the phosphodiester bond.

the site, it shows several important structural features that may relate to CPT activity.

In the structural model shown in Figure 4, both the 10- and 11-positions point out toward the sugar backbone, whereas the 9-position is in the minor groove. This model suggests that electron-rich groups of moderate size would be favored for both the 10- and 11-positions, whereas the 9-position could bear a bulky group. Twelve A ring substituted compounds were evaluated in our modeling studies. Our own anlysis indicates that bulk tolerance at position 10 is limited and that derivatives with flexible side chains capable of occupying space in the plane of the A ring are able to produce enzyme-mediated DNA cleavage, whereas derivatives with side chains that protrude above or below the plane of the A ring are much less active. This finding is supported by a number of structure−activity relationship studies.[10,14,15,21,45−47] As to the 12-position, our model predicts that a substituent would localize near the DNA major groove. The inactivaty of such derivatives[15] as top1 inhibitors may be related to steric hindrance by the top1 peptide located in the DNA major groove.

We have been particularly interested in comparing the structural model of 10,11-methylenedioxy (MDO) CPT with that of 10,11-dimethoxy (DMO) CPT, because of the essential chemical similarity of these two CPT derivatives, despite the strong activity of the former and

Table 3. Conformational Energies of 10,11-Dimethoxy CPT

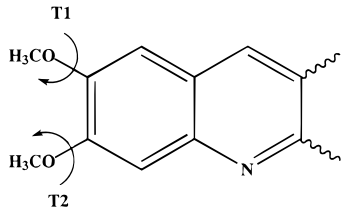

comformer	T1	T2	*E* (kcal/mol)	choice
4_1	−0.8	−0.6	44.529	exclude
4_2	−0.4	−145.1	46.423	use
4_3	−148.7	0.0	46.436	exclude
4_4	−111.2	−111.6	47.022	use
4_5	112.1	112.1	47.165	use

lack of activity of the latter.[14,15] To provide a structural explanation for MDO activity and DMO inactivity, it is useful to consider the rotational barrier of C−O−C═C of 10,11-DMO CPT. Anisole is a compound containing the same structural fragment as part (the A ring) of 10,-11-DMO CPT. The C−O−C═C barrier in this molecule has been studied experimentally[48−50] and by ab initio calculations.[51] The experimental values have varied from 1.30 to 5.22 kcal/mol, but the most recently reported experiments gave a value of 2.26 kcal/mol.[49] This barrier was calculated to be 2.39 kcal/mol by an ab initio method using the 6-31G basis set with inclusion of electron correlation.[51] We obtain a value of 2.03 kcal/mol in the modified AMBER force field, in good agreement with the reported experimental and calculated values. There appear to be five possible conformers of 10,11-DMO CPT in terms of the orientations of two methoxy groups (see Table 3). The least stable of these conformers has an energy 2.64 kcal/mol higher than that of the most stable one. However, the lower energy conformers 4_1 and 4_3 are excluded according to our premise that substituents encroaching upon space in the vicinity of position 12 would block interaction with the binding site. Three other conformers were docked into the binding site to form complexes 4_2, 4_4, and 4_5 (see Tables 2 and 3). Two destabilizing factors are reflected in the ternary cleavable complex model with 10,11-DMO CPT: (i) unfavorable stacking interaction and (ii) steric misfit in the DNA−top1 binding pocket. Drug stacking in the complex is somewhat perturbed by the two aliphatic methoxy groups. In contrast, the stacking forces between superposed and parallel aromatic ring structures in the ternary cleavable complex of 10,11-MDO CPT should be stronger. A large steric repulsion between the two methoxy groups of 10,11-DMO CPT and the DNA base pairs of nucleotides is also observed, especially in complex 4_5. This repulsion prevents the "intercalation" of 10,11-DMO CPT into the critical region of the binding site (see Figure 5). In contrast, as shown in Figure 5, the substituent atoms of 10,11-MDO CPT are tied together in an almost planar ring, creating a sterically favorable environment for "intercalation" of 10,11-MDO CPT into the binding site.

To further examine the "bulk tolerance limit" at C-10, we investigated four other substituted methylenedioxy (MDO) and ethylenedioxy (EDO) camptothecins (compounds **7**−**8**, **10**−**11** shown in Figure 2) which were reported to be more potent than CPT.[15,28,29,43,47] According to our modeling studies, the substituents at the

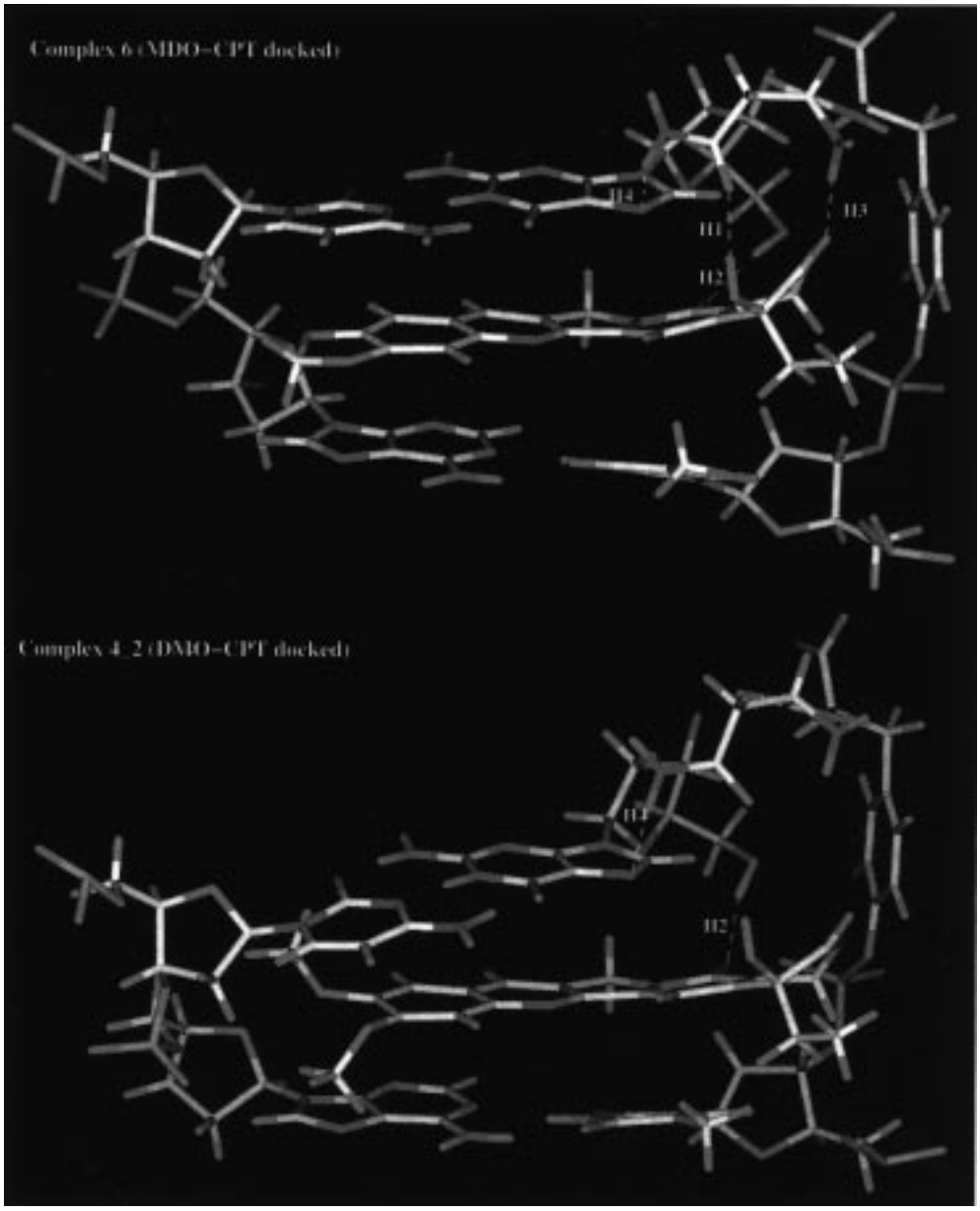

Figure 5. Hypothetical complexes of MDO CPT and DMO CPT with top1 and DNA. MDO CPT fits better than DMO CPT (H1−H4 are defined in Figure 6).

A ring appeared compact, and these four compounds all showed much more favorable interactions than CPT with the binary DNA−top1 complex (see Table 2). They fitted into the hypothetical binding site, and the methylhydroxyl or methylamino substituent on the ethylenedioxy ring was able to form a hydrogen bond to the oxygen of the phosphodiester bond.

A series of 11-aza-20*S*-camptothecin analogues have been synthesized and tested by other investigators[52] using the top1 enzyme cleavage complex assay. We analyzed these compounds using our hypothetical binding site model and found that the compounds with small substituents at C-10 or with a substituent at C-10 capable of forming hydrogen bonds showed relatively high interaction energies. The results for three interesting 11-aza camptothecin analogues (compounds **16**−**18** in Figure 2) are presented in Table 2. These 11-aza 20*S*-CPT analogues have been reported to be more potent top1 inhibitors than CPT.[52] Especially potent were compounds **17** and **18**, which are almost as active as 10,11-MDO 20*S*-CPT. The same trend was observed in the modeling studies in terms of their interaction energies.

There are limitations in the precise calculation of the interaction energies of these complexes. Most prominently, we cannot model well the interactions of the A ring with the hypothetical binding site because the complete structural information very recently reported[53,54] was not yet available. This limitation could account for errors in calculating the exact interaction energies despite other factors such as entropy changes, solvent effects, and stacking interactions. This difficulty is reflected in the calculated energies of compound 6, 10,11-MDO-20*S*-CPT. In our calculation, compound **6** has almost the same interaction energies as compound **3**, but the former has much lower IC_{50} values in the DNA cleavage assay.

6. Possible Hydrogen Bonding Site Near the E Ring. It is well-known that the relative positions and distances between hydrogen bond accepting and donat-

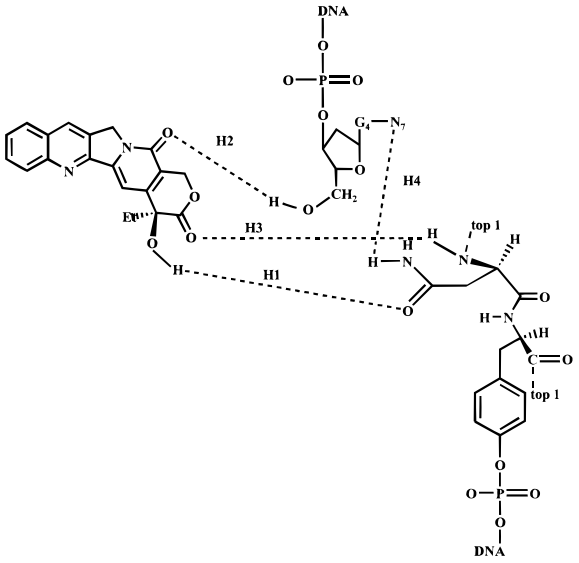

Figure 6. Hypothesized hydrogen binding sites in the ternary cleavable complex.

ing sites are critical for effective recognition and binding of ligands. Studying the three-dimensional structural model, we postulated four possible hydrogen bonds in a region near the E ring in the binding site, as shown in Figure 6. These hydrogen-bonding interactions between CPT and the DNA−top1 binding site were accorded special attention because the lactone portion and the 20*S* configuration of the E ring have been shown experimentally to be critical for top1 inhibition by CPT.[14,15,26] The distances between these pairs of atoms in 16 hypothetical complexes are summarized in Table 2. When the active and inactive CPT analogues are compared, the hydrogen-bonding interactions do appear to be important in the binding of CPT with DNA−top1. Thus, hydrogen bonds may account, in large part, for stabilization of the ternary cleavable complex. Two of them (H1 and H3) reflect interactions between the CPT and top1, and one of them (H2) reflects interaction between the CPT and 5′ DNA terminal hydroxyl of the top1 break. There is also a strong hydrogen bond interaction (H4) between the asparagine side chain amino group and the N7 position of guanine. These specific interactions (H2 and H4) agree with the early experimental hypothesis that camptothecin interacts with the base (preferentially guanine) at the 5′ DNA terminus of the top1 break (position +1).[12,16] The correspondence between the inactivity of compounds **10**−**12** (see Table 2) and unfavorable interactions also strengthens the possibility that these hydrogen-bonding patterns are important.

On the basis of the experimental evidence, two possible reasons can be proposed for the importance of the CPT 20-hydroxyl group in the *S* configuration for top1 inhibition: (1) the formation of a hydrogen bond between the hydroxyl group and the enzyme−DNA complex; (2) the presence of an intramolecular hydrogen bond with the lactone carbonyl of CPT (21 position). Both interactions might facilitate the possible "E ring opening" reaction.[14,19,20,22,46] This process might be critical for top1 inhibition following noncovalent ternary cleavable complex formation with the closed form of the lactone ring.[14,55]

In our computational model shown in Figure 6, the 20-hydroxyl hydrogen bonds to the asparagine carbonyl oxygen in top1, rather than to the carbonyl oxygen at C-21 of the E ring of CPT. If we assume that "enzyme-stabilized" lactone ring opening is possible, this hydrogen bond could assume proper geometric orientation of the carbonyl group in the 21-position for attack by a nucleophile in top1. As a result of the hydrogen-bonding interactions (H1 and H3 shown in Figure 6), the indirect and direct electron shifting effects make the carbonyl carbon more electrophilic and would facilitate a ring-opening reaction. We further examined the stability of the complex after E ring opening. The hydroxyl formed at position 21 was observed to hydrogen bond with the phosphate oxygen of the cytidine nucleotide (reactive site) in the binding site after E ring opening. This hydrogen bond would stabilize the ternary cleavable complex further, while the 20-hydroxyl could still hydrogen bond to the carbonyl oxygen of the asparagine. This modeling result corresponds to an experiment-

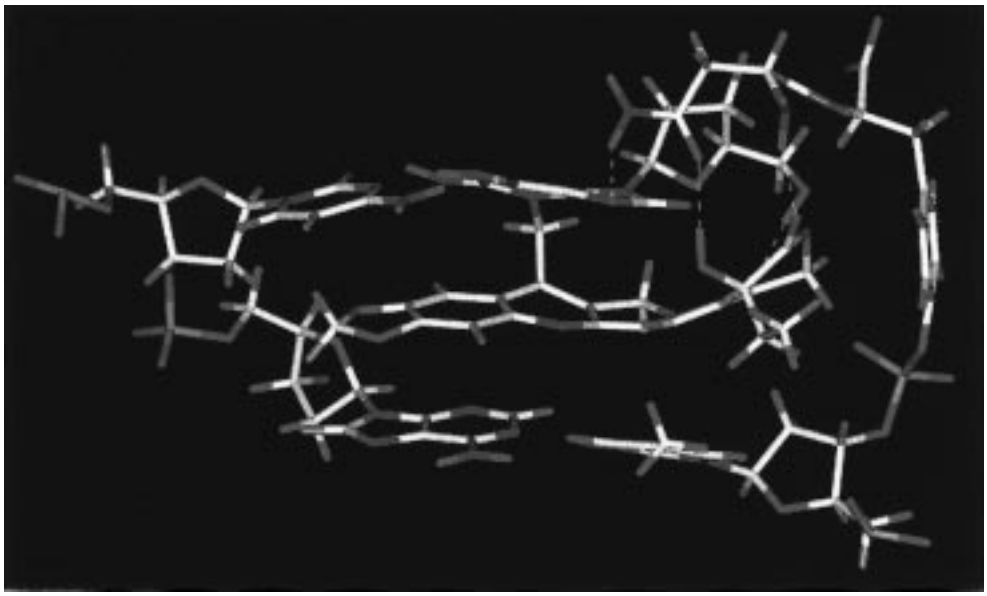

Figure 7. Hypothetical model of DNA alkylation by 7-chloromethyl 10,11-MDO CPT.

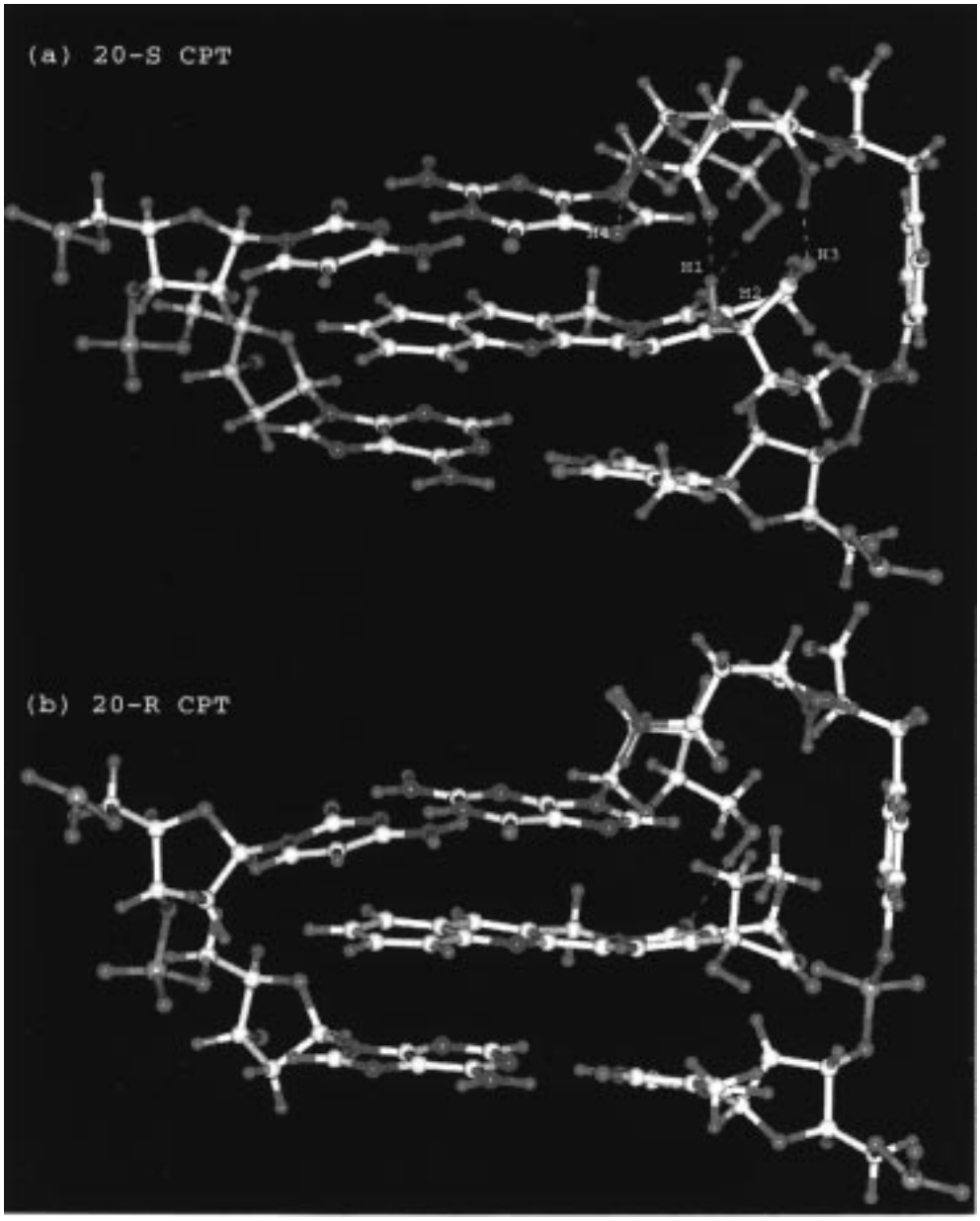

Figure 8. The best energy minimized structures of ternary cleavable complexes with (a) 20*S* CPT and (b) 20*R* CPT.

based speculation[14] that a hydrogen bond can form between the 20-hydroxyl group and the enzyme−DNA complex.

The model does not directly account for the observation that replacement of the 21-lactone by a 21-lactam causes a loss of activity. The 21-lactone CPT and 21-lactam CPT form very similar stacking models and hydrogen-bonding frameworks in the hypothetical binding site, and they are very similar in interaction energies. If we assumed that "enzyme-stabilized lactone ring opening" is the second step for top1 inhibition, the inactivity of 21-lactam CPT might be explained by the fact that lactam ring opening does not occur as readily as does lactone ring opening. We are aware that 21-thiolactone CPT is also inactive, whereas it would be expected to be as reactive as 21-lactone CPT in the ring opening. Although we cannot give a definite reason for the inactivity of 21-thiolactone CPT, one speculation is that the weaker electronegativity of sulfur than of oxygen could help to destabilize the covalent complex. This difference might shift the equilibrium toward ring closure in the presumed reversible process.

7. 20*S* CPT and Its Inactive 20*R* Enantiomer. Camptothecin has an asymmetric carbon at position 20. The natural 20*S* CPT is approximately 2-fold more potent than a racemic mixture of synthetic 20*S* and 20*R* CPT, and 20*R* CPT is inactive as a top1 inhibitor.[14,15]

This difference may be explained by the postulated model structures (Figure 8 and Table 2). The model for DNA−top1 complexation with 20*S* CPT includes three hydrogen bonds (H1−H3) between CPT and the postulated binding site. Two of these (H1 and H3) are absent in the corresponding 20*R* CPT complex. This absence could decrease the stability of the ternary cleavable complex. In addition, the carbonyl group in the lactone ring of docked 20*R* CPT is also less accessible to nucleophile in top1. Both the geometrical features and the electronic effects suggest that 20*R* CPT might not undergo E ring opening and closure reactions as readily as does 20*S* CPT. Our model is thus consistent with

the stereospecificity of CPT activity in terms of a stereospecific binding in the ternary cleavable complex.

8. Resistance to CPT. Mutations in the TOP1 gene, which can reduce the ability of CPT to stabilize cleavable complexes is one of the possible mechanisms of CPT resistance.[1] A CPT-resistant cell line, CEM/C2, was derived from the human leukemia cell line CCRF-CEM.[26,27,56] The resistance is due to the mutation Asn722Ser, which is next to the catalytic tyrosine 723. Substitution of leucine for this amino acid residue immediately N-terminal to the catalytic tyrosine also results in CPT resistance.[57] The amino acid sequence of this region is highly conserved among eukaryotic top1's from different organisms.[1]

We used our three-dimensional model to elucidate the possible mechanism of this resistance. Torsional angles of the tyrosine and peptide backbone in mutant top1 were assumed to be the same as those in wild-type top1 except for the serine side chain. The interaction energy for complex **19** (Table 2) was calculated from the model, along with the nonbonded distances between potential hydrogen bond donating and accepting groups described earlier in this paper. The hypothetical ternary cleavable complex structure with the mutant top1 is energetically less favorable than is that with wild-type top1, as a result of relatively unfavorable electrostatic and hydrogen bonding interactions. The side chain hydroxyl of serine is a potential hydrogen bond donating or accepting group, but it cannot form a hydrogen bond with the CPT 20-hydroxyl as does the asparagine amide oxygen. Instead, the CPT 20-hydroxyl hydrogen can form a hydrogen bond with N7 at G+1. In addition, the strong hydrogen bond interaction (H4 in the wild-type top1 model) between the asparagine side chain amino group and the N7 position of guanine does not exist in the mutant top1 ternary cleavable complex. These unpaired donors or acceptors in the ternary cleavable complex with mutant top1, as reflected in a reduction in the number of hydrogen bonds in the bound state, create an unfavorable electrostatic environment. Thus, our model is consistent with the possibility that the Asn722Ser mutant form of top1 lacks the stabilizing electrostatic interactions for CPT binding.

Conclusion

For the presumed ternary cleavable complex, we have developed a three-dimensional structural model consistent with a number of experimental observations. The model was first validated by the observation that 7-ClMe-MDO-CPT could alkylate the N3 position of the purine +1 adjacent to the top1 cleavage site, and in terms of the relative potencies of eighteen CPT ligands. It is also consistent with the camptothecin resistance observed for the Asn722Ser top1 mutation.

According to the model, CPT interacts with DNA and with top1 near its catalytic tyrosine. This binding is stabilized by stacking and by a set of proposed hydrogen bonding interactions in the binding site. Both our model and the recently published model of Redinbo et al.[53] postulate the stacking of CPT with the +1 purine. However, the model of Redinbo et al.[53] differs from ours because it proposes the following: (i) the +1 purine is displaced outside of the DNA duplex in the presence of CPT, (ii) CPT binds to the DNA helix in the place of the +1 purine and is also stacked with the +1 purine externally from the duplex DNA structure, and (iii) the terminal carbon (C-18) of the CPT ethyl group must be rotated slightly relative to its position in the CPT crystal structure[35] to remove steric clashes with the side chain of Asp[533] and the −1 base.[53] The structural models presented here and by Redinbo et al.[53] are both plausible but by no means proven. They provides a concrete basis for further structural studies and for the generation and testing of novel top1 inhibitors.

Acknowledgment. The authors thank Dr. Michael Chen of the Department of Chemistry at the University of Georgia for many valuable suggestions during the course of this work. We also thank Dr. Peter Fox of Tripos Associates, Inc. for frequent assistance.

References

(1) Gupta, M.; Fujimori, A.; Pommier, Y. Eukaryotic DNA topoisomerase I. *Biochim. Biophys. Acta* **1995**, *1262*, 1−14.
(2) Wang, J. C. DNA topoisomerases. *Annu. Rev. Biochem*. **1996**, *65*, 635−692.
(3) Champoux, J. *Mechanistic aspects of type-I topoisomerase;* Cold Spring Harbor Laboratory: Cold Spring, 1990.
(4) Chen, A. Y.; Liu, L. F. DNA topoisomerases: essential enzymes and lethal targets. *Annu. Rev. Pharmacol. Toxicol*. **1994**, *94*, 194−218.
(5) Hsiang, Y. H.; Hertzberg, R.; Hecht, S.; Liu, L. F. Camptothecin induces protein- linked DNA breaks via mammalian DNA topoisomerase I. *J. Biol. Chem*. **1985**, *260*, 14873−14878.
(6) Pommier, Y. Eukaryotic DNA topoisomerase I: genome gate keeper and its intruders, camptothecins. *Sem. Oncol*. **1996**, *23*, 1−10.
(7) Slichenmyer, W. J.; Rowinsky, E. K.; Donehower, R. C.; Kaufmann, S. H. The current status of camptothecin analogues as antitumor agents. *J. Natl. Cancer Inst*. **1993**, *85*, 271−287.
(8) Rothenberg, M. L. Topoisomerase I inhibitors: review and update. *Ann. Oncol*. **1997**, *8*, 837−855.
(9) Leteurtre, F.; Fesen, M.; Kohlhagen, G.; Kohn, K. W.; Pommier, Y. Specific interaction of camptothecin, a topoisomerase I inhibitor, with guanine residues of DNA detected by photoactivation at 365 nm. *Biochemistry* **1993**, *32*, 8955−8962.
(10) Hertzberg, R. P.; Caranfa, M. J.; Hecht, S. M. On the mechanism of topoisomerase I inhibition by camptothecin evidence for binding to an enzyme-DNA complex. *Biochemistry* **1989**, *28*, 4629−4638.
(11) Pommier, Y.; Kohlhagen, G.; Kohn, K. W.; Leteurtre, F.; Wani, M. C.; Wall, M. E. Interaction of an alkylating camptothecin derivative with a DNA base at topoisomerase I-DNA cleavage sites. *Proc. Natl. Acad. Sci. U.S.A*. **1995**, *92*, 8861−8865.
(12) Jaxel, C.; Capranico, G.; Kerrigan, D.; Kohn, K. W.; Pommier, Y. Effect of local DNA sequence on topoisomerase I cleavage in the presence or absence of camptothecin. *J. Biol. Chem*. **1991**, *266*, 20418−20423.
(13) Wall, M. E.; Wani, M. C. Camptothecin and taxol: discovery to clinic— thirteenth Bruce F. Cain Memorial Award Lecture. *Cancer Res*. **1995**, *55*, 753- 760.
(14) Pommier, Y.; Jaxel, C.; Heise, C. R.; Kerrigan, D.; Kohn, K. W. *Structure- activity relationship by camptothecin derivatives: evidence for the existence of a ternary cleavable complex*; Oxford University Press: New York, 1991.
(15) Jaxel, C.; Kohn, K. W.; Wani, M. C.; Wall, M. E.; Pommier, Y. Structure−activity study of the actions of camptothecin derivatives on mammalian topoisomerase 1: Evidence for a specific receptor site and a relation to antitumor activity. *Cancer Res*. **1989**, *49*, 1465−1469.
(16) Tanizawa, A.; Kohn, K. W.; Pommier, Y. Induction of cleavage in topoisomerase I cDNA by topoisomerase I enzymes from calf thymus and wheat germ in the presence and absence of camptothecin. *Nucl. Acids Res*. **1993**, *21*, 5157−5166.
(17) Porter, S. E.; Champoux, J. J. The basis for camptothecin enhancement of DNA breakage by eukaryotic topoisomerase I. *Nucl. acids Res*. **1989**, *17*, 8521−8532.
(18) Svejstrup, J. Q.; Christiansen, K.; Gromova, I. I.; Anderson, A. H.; Westergaard, O. New technique for uncoupling the cleavage and religation reactions of eukaryotic topoisomerase I. The mode of action of camptothecin at a specific recognition site. *J. Mol. Biol*. **1991**, *222*, 669−678.
(19) Crow, R. T.; Crothers, D. M. Structural modifications of camptothecin and effects on topoisomerase I inhibition. *J. Med. Chem*. **1992**, *35*, 4160−4164.

(20) Pommier, Y.; Tanizawa, A.; Kohn, K. W. Mechanisms of topoisomerase I inhibition by anticancer drugs. *Adv. Pharmacol.* **1994**, *29B*, 73−91.
(21) Hertzberg, R. P.; Busby, R. W.; Caranfa, M. J.; Holden, K. G.; Johnson, R. K.; Hecht, S. M.; Kingsbury, W. D. Irreversible trapping of the DNA-topoisomerase I covalent complex. *J. Biol. Chem.* **1990**, *265*, 19287−19295.
(22) Hertzberg, R. P.; Caranfa, M. J.; Holden, K. G.; Jakas, D. R.; Gallagher, G.; Mattern, M. R.; Mong, S. M.; Bartus, J. O.; Johnson, R. K.; Kingsbury, W. D. Modification of the hydroxy lactone ring of camptothecin: inhibition of mammalian topoisomerase I and biological activity. *J. Med. Chem.* **1989**, *32*, 2, 715−720.
(23) Kingsbury, W. D.; Boehm, J. C.; Jakas, D. R.; Holden, K. G.; Hecht, S. M.; Gallagher, R. P. Synthesis of water-soluble (aminoalkyl)camptothecin analogues: Inhibition of topoisomerase 1 and antitumor activity. *J. Med. Chem.* **1991**, *34*, 98−107.
(24) Sawada, S.; Nokata, K.; Furuta, T.; Yokokura, T.; Miyasaka, T. Chemical modification of an antitumor alkaloid camptothecin synthesis and antitumor activity of 7-C substituted camptothecins. *Chem. Pharm. Bull.* **1991**, *39*, 2574- 2580.
(25) Emerson, D. L.; Besterman, J. M.; Brown, H. R.; Evans, M. G.; Leitner, P. P.; Luzzio, M. J.; Shaffer, J. E.; Sternbach, D. D.; Uehling, D.; Vuong, A. In vivo antitumor activity of two new seven-substituted water-soluble camptothecin analogues. *Cancer Res.* **1995**, *55*, 603−609.
(26) Hsiang, Y.-H.; Liu, L. F.; Wall, M. E.; Wani, M. C.; Nicholas, A. W.; Manikumar, G.; Kirschenbaum, S.; Silber, R.; Potmesil, M. DNA topoisomerase 1-mediated DNA cleavage and cytotoxicity of camptothecin analogs. *Cancer Res.* **1989**, *49*, 9, 4385−4389.
(27) Fujimori, A.; Harker, W. G.; Kohlhagen, G.; Hoki, Y.; Pommier, Y. Mutation at the catalytic site of topoisomerase I in CEM/C2, a human leukemia cell line resistant to camptothecin. *Cancer Res.* **1995**, *55*, 1339−1346.
(28) Evans, M. G. *Chiral Benzdioxane camptothecins as water-soluble topoisomerase I inhibitors*; American Chemical Society Meeting, 1994; p 52.
(29) Milstead, M. W. *Substituted methylenedioxy camptothecins as water-soluble topoisomerase I inhibitors*; American Chemical Society Meeting, 1994; p 51.
(30) Weiner, S. J.; Kollman, P. A.; Case, D. A.; Singh, U. C.; Ghio, C.; Alagona, G.; Profeta, S.; Weiner, P. A new force field for molecular mechanical simulation of nucleic acids and proteins. *J. Am. Chem. Soc.* **1984**, *106*, 765−784.
(31) Weiner, P. K.; Kollman, P. A. AMBER: assisted model building with energy refinementA general program for modeling molecules and their interactions. *J. Comput. Chem.* **1981**, 287−303.
(32) Tripos Associates. *Sybyl Molecular Modeling Software, Sybyl theory manual*; , 6.1 ed.; Tripos Associates, St. Louis, 1994.
(33) Padlan, E. A.; Kabat, E. A. Modeling of antibody complex. *Methods Enzymol.* **1991**, *203*, 3-21.
(34) Rini, J. M.; Schulze-Gahmen, U.; Wilson, I. A. Structural evidence for induced fit as a mechanism for antibody-antigen recognition. *Science* **1992**, *255*, 959−965.
(35) McPhail, A. T.; Sim, G. A. The structure of camptothecin: X-ray analysis of camptothecin iodoacetate. *J. Chem. Soc. B* **1968**, 923−928.
(36) Sarai, A.; Mazur, J.; Nussinov, R.; Jernigan, R. L. Origin of DNA helical structure and its sequence dependence. *Biochemistry* **1988**, *27*, 8498−8502.
(37) Sponer, J.; Kypr, J. Relationships among rise, cup, roll and stagger in DNA suggested by empirical potential studies of base stacking. *J. Biomol. Struct. Dyn.* **1993**, *11*, 27−41.
(38) Dickerson, R. E. Base sequence and helix structure variation in B and A DNA. *J. Mol. Biol.* **1983**, *166*, 419−441.
(39) Sponer, J.; Hobza, P. Bifurcated hydrogen bonds in DNA crystal structures. An *ab initio* quantum chemical study. *J. Am. Chem. Soc.* **1994**, *116*, 709−714.
(40) Hunter, C. A. Sequence-dependent DNA structure. The role of base stacking interactions. *J. Mol. Biol.* **1993**, *230*, 1025−1054.
(41) Price, S. L.; Stone, A. J. The electrostatic interactions in van der Waals complexes involving aromatic molecules. *J. Chem. Phys.* **1987**, *86*, 2859−2868.
(42) Covey, J. M.; Jaxel, C.; Kohn, K. W.; Pommier, Y. Protein-linked DNA strand breaks induced in Mammalian cells by camptothecin, an inhibitor of topoisomerase I. *Cancer Res.* **1989**, *49*, 5016−5022.
(43) Valenti, M.; Nieves-Neira, W.; Kohlhagen, G.; Kohn, K. W.; Wall, M. E.; Wani, M. C.; Pommier, Y. Novel 7-alkyl methylenedioxy-camptothecin derivatives exhibit increased cytotoxicity and induce persistent cleavable complexes both with purified mammalian topoisomerase I and in human colon carcinoma SW620 cells. *Mol. Pharmacol.* **1997**, *52*, 82−87.
(44) Tanizawa, A.; Kohn, K. W.; Kohlhagen, G.; Leteurte, F.; Pommier, Y. Differential stabilization of eukaryotic DNA topoisomerase I cleavable complexes by camptothecin derivatives. *Biochemistry* **1995**, *34*, 7200−7206.
(45) Peel, M. R.; Milstead, M. W.; Sternbach, D. D.; Besterman, J. M.; Leitner, P.; Morton, B. Noverl A-ring modified camptothecins as topoisomerase I inhibitors. *Bioorg. Med. Chem. Lett.* **1995**, *5*, 2129−2132.
(46) Yaegashi, T.; Sawada, S.; Nagata, H.; Furuta, T.; Yokokura, T.; Miyasaka, T. Synthesis and antitumor activity of 20(S)-camptothecin derivatives. A-ring-substituted 7-methyl camptothecin and their E-ring modified water-soluble derivatives. *Chem. Pharm. Bull.* **1994**, *42*, 2518−2525.
(47) Luzzio, M. J.; Besterman, J. M.; Emerson, D. L.; Evans, M. G.; Lackey, K.; Leitner, P. L.; McIntyre, G.; Morton, B.; Myers, P. L.; Peel, M.; Sisco, J. M.; Sternbach, D. D.; Tong, W.-Q.; Truesdale, A.; Uehling, D. E.; Vuong, A.; Yates, J. Synthesis and antitumor activity of novel water-soluable derivatives of camptothecin as specific inhibitors of topoisomerase I. *J. Med. Chem.* **1995**, *38*, 395−401.
(48) Owen, N. L.; Hester, R. E. Vibrational spectra and torsional barriers of anisole and some monohalogen derivatives. *Spectrochim. Acta* **1969**, *25A*, 343−354.
(49) Grindley, T. B.; Katrizky, A. R.; Topsom, R. D. Infrared intensities as a quantitative measure of intramolecular interactions. Part XXXIV. Quantitative relations between conjugation and strain energies and s_R values: rotational barriers in monosubstituted benzenes. *J. Chem. Soc., Perkin Trans. 2* **1974**, 289−297.
(50) Garg, S. K.; Smyth, C. D. Microwave absorption and molecular structure in liquids. LXVIII. Dielectric behavior at 2.2-mm wavelength and intramolecular motion in five substituted benzenes and cyclohexanes. *J. Chem. Phys.* **1967**, *46*, 373−377.
(51) Vincent, M. A.; Hiller, I. H. A theoretical study of methoxy group rotation in anisole. *Chem. Phys.* **1990**, *140*, 35−40.
(52) Uehling, D. E.; Nanthakumar, S. S.; Croom, D.; Emerson, D. L.; Leitner, P. P.; Luzzio, M. J.; McIntyre, G.; Morton, B.; Profeta, S.; Sisco, J.; Sternbach, D. D.; Tong, W.-W.; Vuong, A.; Besterman, J. M. Synthesis, topoisomerase I inhibitory activity, and in vivo evaluation of 11-azacamptothecin analogs. *J. Med. Che*m. **1995**, *38*, 1106−1118.
(53) Redinbo, M. R.; Stewart, L.; Kuhn, P.; Champoux, J. J.; Hol, W. G. J. Crystal structure of human topoisomerase I in covalent and noncovalent complexes with DNA. *Science* **1998**, *279*, 1504−1513.
(54) Stewart, L.; Redinbo, M. R.; Qiu, X.; Hol, W. G. J.; Champoux, J. J. A model for the mechanism of human topoisomerase I. *Science* **1998**, *279*, 1534−1541.
(55) Nicholas, A. W.; Wani, M. C.; Manikumar, G.; Wall, M. E.; Kohn, K. W.; Pommier, Y. Plant antitumor agents 29. Synthesis and biological activity of ring D and ring E modified analogues of camptothecin. *J. Med. Chem.* **1990**, *33*, 972−978.
(56) Fujimori, A.; Hoki, Y.; Popescu, N.; Pommier, Y. Silencing and selective methylation of the normal topoisomerase I gene in camptothecin-resistant CEM/C2 human leukemia cells. *Oncol. Res.* **1996**, *295−301*.
(57) Knab, A. M.; Fertala, J.; Bjornsti, M.-A. Mechanisms of camptothecin resistance in yeast DNA topoisomerase I mutants. *J. Biol. Chem.* **1993**, *268*, 22322−22330.

JM9605445